Drug Metabolism and Pharmacokinetics 30 (2015) 174–181

Contents lists available at ScienceDirect

Drug Metabolism and Pharmacokinetics

journal homepage: http://www.journals.elsevier.com/drug-metabolism-and-pharmacokinetics

Regular article

Inhibition effects of *Vernonia cinerea* active compounds against cytochrome P450 2A6 and human monoamine oxidases, possible targets for reduction of tobacco dependence

Aruna Prasopthum [a], Phisit Pouyfung [a], Songklod Sarapusit [b], Ekaruth Srisook [c], Pornpimol Rongnoparut [a, *]

[a] *Department of Biochemistry, Faculty of Science, Mahidol University, 272 Rama 6 Rd., Ratchathewi, Bangkok 10400, Thailand*
[b] *Department of Biochemistry, Faculty of Science, Burapha University, 169 Long-Hard Bangsaen Rd., Mueang, Chonburi 20131, Thailand*
[c] *Department of Chemistry and Center for Innovation in Chemistry, Faculty of Science, Burapha University, 169 Long-Hard Bangsaen Rd., Mueang, Chonburi 20131, Thailand*

ARTICLE INFO

Article history:
Received 30 September 2014
Received in revised form
25 November 2014
Accepted 21 December 2014
Available online 2 January 2015

Keywords:
P450 2A6
MAO
Vernonia cinerea
Flavonoids
Hirsutinolides

ABSTRACT

The human cytochrome P450 2A6 (CYP2A6) and monoamine oxidases (MAO-A and MAO-B), catalyzing nicotine and dopamine metabolisms, respectively, are two therapeutic targets of nicotine dependence. *Vernonia cinerea*, a medicinal plant commonly used for treatment of diseases such as asthma and bronchitis, has been shown reducing tobacco dependence effect among tobacco users. In the present study, we found eight active compounds isolated from *V. cinerea* that comprise inhibitory activity toward CYP2A6 and MAO-A and MAO-B enzymes using activity-guided assays, with coumarin as substrate of CYP2A6 and kynuramine of MAOs. These compounds were three flavones (apigenin, chrysoeriol, luteolin), one flavonol (quercetin), and four hirsutinolide-type sesquiterpene lactones (8α-(2-methylacryloyloxy)-hirsutinolide-13-*O*-acetate, 8α-(4-hydroxymethacryloyloxy)-hirsutinolide-13-*O*-acetate, 8α-tigloyloxyhirsutinolide-13-*O*-acetate, and 8α-(4-hydroxytigloyloxy)-hirsutinolide-13-*O*-acetate). Modes and kinetics of inhibition against the three enzymes were determined. Flavonoids possessed strong inhibitory effect on CYP2A6 in reversible mode, while inhibition by hirsutinolides was mechanism-based (NADPH-, concentration-, and time-dependence) and irreversible. Inhibition by hirsutinolides could not be reversed by dialysis and by addition of trapping agents or potassium ferricyanide. Flavonoids inhibited MAOs with variable degrees and were more prominent in inhibition toward MAO-A than hirsutinolides, while two of hirsutinolides inhibited MAO-B approximately comparable to two flavonoids. These results could have implications in combination of drug therapy for smoking cessation.

1. Introduction

Tobacco smoking and dependence is a world-wide health problem, causing adverse health effects and many tobacco-related diseases. Nicotine is the main addictive compound in tobacco and addiction to nicotine produces prolonged smoking, causing smokers expose to many other deleterious ingredients in tobacco and tobacco smoke [1]. When inhaled, nicotine quickly enters systemic circulation and brain via diffusion into pulmonary blood. The human liver cytochrome P450 (CYP) 2A6, a heme-containing enzyme in the cytochrome P450 monooxygenase superfamily, is the primary enzyme that metabolizes nicotine absorbed into the body [2]. Moreover, CYP2A6 mediates activation of tobacco-specific carcinogenic compounds such as 4-(methylnitrosamino)-1-(3-pyridyl)-1-butanone (NNK) and contributes to increased risks of lung cancer and respiratory diseases among smokers [3]. In the brain, nicotine binds to nicotinic cholinergic receptors and stimulates dopaminergic neurons in the mesolimbic brain reward pathways, leading to an increased release of dopamine that plays a key role in reward mechanisms in tobacco users [1]. Dopamine is metabolized by the mitochondrial monoamine oxidases (MAOs) that are present in two isoforms, MAO-A and MAO-B [4]. Inhibition of both MAOs by non-nicotinic chemicals in tobacco smoke (harman and norharman) was observed, potentiating the pleasurable

* Corresponding author.
E-mail address: pornpimol.ron@mahidol.ac.th (P. Rongnoparut).

http://dx.doi.org/10.1016/j.dmpk.2014.12.005

experiences of the brain through increasing dopamine levels [4,5]. Specifically, smoking reduced brain MAO-A by 30% and MAO-B by 40% [4]. Quitting of cigarette smoking causes withdrawal symptoms and is associated with dopamine and MAOs levels [6–8].

Pharmacotherapy for smoking cessation has currently employed nicotine replacement therapy (NRT) and non-nicotinic therapeutic drugs that affect tobacco dependence [9]. Polymorphic variations in the CYP2A6 gene, reflecting variability in rate of nicotine metabolism, have been linked to differences in smoking consumption, vulnerability to addiction, smoking cessation, and lung cancer risks [1,10]. Thus inhibitors of CYP2A6-mediated nicotine metabolism, mimicking CYP2A6 gene defect, are suggested candidates for smoking reduction and decreasing risk of exposure to metabolically activated carcinogenic compounds [1,9]. An oral treatment with methoxsalen, a CYP2A6 selective irreversible inhibitor has shown decreases of cigarette smoking through inhibition of nicotine metabolism [11,12]. Moreover medications that could help stabilizing dopamine level through inhibition of MAO during tobacco withdrawal have been proposed as a treatment for tobacco dependence [8]. Oral administration of selegiline, an irreversible MAO-B inhibitor, and combination of oral selegiline and NRT showed a trend in decreased tobacco craving during tobacco abstinence compared to placebo [13–15]. Moclobemide, a reversible MAO-A inhibitor, has also been reported facilitating smoking cessation and abstinence in heavy, dependent smokers [16]. Thus compounds that are inhibitors of CYP2A6-mediated nicotine metabolism and MAOs that attenuate the reinforcing properties of nicotine might help alleviating withdrawal symptoms during smoking cessation.

Vernonia cinerea Less (Asteraceae) is a perennial herbaceous plant, widely used in traditional medicine in India, Africa and Asia. It is commonly used for treatment of various diseases such as worm and skin diseases, asthma, bronchitis, cough [17]. Various pharmacological activities have been reported for *V. cinerea* including analgesic, anti-pyretic, and anti-inflammatory activities [18]. Recently, *V. cinerea* prepared as herbal tea has shown smoking abstinence effects in smokers [19]. Supplementation of *V. cinerea* preparations with exercise could reduce smoking rate in smokers in relation to oxidative stress and beta-endorphin levels in smokers [20]. These results imply that *V. cinerea* comprises compounds that help reducing smoking and sustaining smoking abstinence during smoking cessation. Phytochemical analysis of *V. cinerea* showed the presence of steroids, sesquiterpenes, and flavonoids [17]. However bioactive compounds in *V. cinerea* involved in smoking abstinence have not been reported.

In this report, we investigated whether there are bioactive compounds in *V. cinerea* that comprise inhibitory activity against the recombinant human CYP2A6, MAO-A and MAO-B enzymes, thereby contributing to reduction of smoking rate previously reported. Coumarin as probe substrate of CYP2A6 and kyuramine of MAOs were employed in the fluorescence-based enzymatic assays. We isolated and identified three flavones, one flavonol and four hirsutinolide-type sesquiterpene lactones from *V. cinerea* that exerted inhibition effects. Kinetics and modes of inhibition of the purified compounds against CYP2A6 and MAOs were determined.

2. Materials and methods

2.1. Chemicals

Coumarin, *R*-(−)deprenyl hydrochloride, kynuramine hydrobromide, 4-hydroxyquinoline, 7-hydroxycoumarin, 1,2-dilauroyl-rac-glycero-3-phosphocholine (DLPC), nicotinamide adenosine diphosphate reduced form (NADPH), methoxsalen, δ-aminolevulinic acid (δ-ALA), isopropyl-beta-D-thiogalactopyranoside (IPTG), phenylmethylsulfonyl fluoride (PMSF), glutathione (GSH), catalase, potassium ferricyanide, and Sephadex LH-20 gel were purchased from Sigma–Aldrich (St. Louis, MO). Silica gel (230–400 mesh) was supplied by Merck (Darmstadt, Germany). Ethyl acetate (EtOAc), hexane, ethanol (EtOH), diethyl ether, chloroform and high performance liquid chromatogryphy (HPLC) grade acetonitrile (ACN) and methanol (MeOH) were obtained from RCI Labscan (Bangkok, Thailand).

2.2. Extraction and isolation of compounds

Aerial parts of *V. cinerea* were obtained from the Chao Krom Poe traditional medicine market, Bangkok, Thailand, in October 2013. The plant materials were identified by Dr. Thaya Jenjittikul, Department of Plant Science, Faculty of Science, Mahidol University, Bangkok, Thailand. A voucher sample (7803) was deposited at Suanluang Rama IX herbarium, Bangkok.

The dry and ground *V. cinerea* material (1 kg) was macerated three times in 95% EtOH (3 × 10 L) at 37 °C, concentrated under reduced pressure at 45 °C to yield 68 g of a viscous mass of ethanol extract. The crude extract was dissolved in 15% EtOH (400 ml) and further partitioned with hexane (3 × 400 ml) and EtOAc (3 × 400 ml), yielding hexane- (17 g), EtOAc- (15 g) and aqueous-soluble extracts (32 g). Stock solutions of both hexane- and EtOAc-soluble extracts (40 mg/ml) were prepared in EtOH and subjected to inhibition assays against CYP2A6 and MAOs enzymes and IC_{50} values determined. To primarily evaluate compounds in the extracts, both hexane and EtOAc extracts were subjected to high performance thin layer chromatography (HPTLC) fingerprint analysis. In brief, samples (2 μl) were spotted on a pre-coated Silica gel 60 F_{254} TLC plate (Merck, Billerica, MA, USA). The plate was developed in diethyl ether: EtOAc (6: 4) and scanned at 254 nm using a CAMAG TLC scanner 3 with Wincats software V1.3.4 (Camag, Muttenz, Switzerland). The R_f values, spectra, λ_{max} and peak areas of the resolved bands were recorded. Relative percentage area of each band was calculated. It was primarily observed from HPTLC analysis that the hexane extract comprised large quantity chlorophylls and chlorophylls contributed to inhibition effects in hexane extract against the three enzymes, thus was not subjected to further compound purification.

To identify active components that inhibited CYP2A6 and MAO enzymes, EtOAc extract was separated by column chromatography over Silica gel (OD 60 mm; 230–400 mesh; 500 g) with successive elution by diethyl ether: EtOAc (100:0 to 0:100). The fractions were collected and pooled according to TLC analysis to afford a total of 12 fractions. All fractions were prepared in EtOH and subjected to inhibition assays against CYP2A6 and MAO-A and MAO-B enzymes. Fractions (10 μg/ml each for CYP2A6 and 100 μg/ml each for MAOs which were approximately 2–3 times IC_{50} values of the EtOH extract) that contained at least 50% inhibition effect were preceded for compound purification.

Fractions 5 (diethyl ether: EtOAc = 1.5: 8.5, 170 mg) and 6 (diethyl ether: EtOAc = 3: 7, 495 mg) were subjected to purification by HPLC (semipreparative RP-18 column; 47.8 mm × 100 mm, Water Corporation, Ireland) with detection at 254 nm. The solvent system (1.5 ml/min) used in HPLC consisted of ACN and water and was set as follows: 0 min, 30% v/v ACN/water; 0–3 min, a linear gradient from 30% to 35% ACN; 3–10 min, 35% ACN; 10–11 min, 35–40% ACN; 11–15 min, 40% ACN; 15–22 min, 40–100% ACN; 22–27 min, 100% ACN; 27–30 min, 100–30% ACN; and 30–35 min, a final equilibration at 30% ACN. The compound in fraction 5 eluted at 11.76 min was identified as apigenin (15.8 mg), and compounds in fraction 6 eluted at 7.98 and 11.63 min were identified as luteolin (102 mg) and chrysoeriol (51 mg), respectively.

Fractions 7, 8 and 9 (diethyl ether: EtOAc = 30–60: 70–40, 2.04 g) of the EtOAc extract were combined and chromatographed on a Silica gel (OD 15 mm; 230–400 mesh; 100 g) and eluted with diethyl ether: EtOAc (20:0 to 0:100) to obtain 7 subfractions (7.1–7.7). Subfractions 7.4 (205 mg), 7.5 (158 mg) and 7.7 (285 mg) exhibiting the strongest inhibitory effect toward CYP2A6 and either MAO-A or MAO-B were subjected to separation on a Sephadex LH-20 gel (25 g) eluted with chloroform: MeOH (2:1) followed by HPLC (semipreparative RP-18 column) with detection at 254 nm. For subfraction 7.4, the mobile phase (1.5 ml/min) was ACN/water and was set as follows: 0–4 min, 45–50% ACN; 4–6 min, 50–55% ACN; 6–15 min, 77–75% ACN; 15–17 min, 75–100% ACN; 17–23 min, 100% ACN; 23–25 min, 100–45% ACN; and 25–30 min, a final equilibration at 45% ACN. Two compounds, 8α-(2-methylacryloyloxy)-hirsutinolide-13-*O*-acetate (23.2 mg) and 8α-tigloyloxyhirsutinolide-13-*O*-acetate (64.5 mg), in subfraction 7.4 were successfully obtained at retention time 20.2 and 21.3 min, respectively. The mobile phase (1.5 ml/min) for separation of subfraction 7.5 was MeOH/water and was set as follows: 0–5 min, 50–70% MeOH; 5–18 min, 70–80% MeOH; 18–20 min, 80–100% MeOH; 20–25 min, 100% MeOH; 25–30 min, 100–50% MeOH; and 30–35 min, a final equilibration at 50% MeOH. Two major peaks in subfraction 7.5 at retention time 7.5 and 8.5 min were obtained as 8α-(4-hydroxymethacryloyloxy)-hirsutinolide-13-*O*-acetate (12.7 mg) and 8α-(4-hydroxytigloyloxy)-hirsutinolide-13-*O*-acetate (6.6 mg), respectively. The mobile phase (1.5 ml/min) for HPLC separation of subfraction 7.7 was ACN/water and HPLC was set similar to separation of fraction 5. A single peak at retention time 2.3 min was obtained as quercetin (19 mg). Elucidation of chemical structures of all purified compounds was based on UV spectra detected on HPLC, electrospray ionization mass spectrometer (ESI-MS/MS, Bruker Daltonics GmbH, Bremen, Germany) in both positive and negative modes and nuclear magnetic resonance (NMR) spectra (Bruker AVANCE 400 MHz NMR Spectrometer, Germany) compared with published literatures [21–26]. Percent yields of four flavonoids from crude ethanol extract were 0.02, 0.08, 0.15 and 0.03 for apigenin, chrysoeriol, luteolin, and quercetin, respectively, and yields of the four hirsutinolides including 8α-(2-methylacryloyloxy)-hirsutinolide-13-*O*-acetate, 8α-(4-hydroxymethacryloyloxy)-hirsutinolide-13-*O*-acetate, 8α-tigloyloxyhirsutinolide-13-*O*-acetate, and 8α-(4-hydroxytigloyloxy)-hirsutinolide-13-*O*-acetate were 0.03%, 0.02% 0.09% and 0.01%, respectively.

2.3. CYP2A6-mediated coumarin 7-hydroxylation assay

The ethanol extract, fractions and purified compounds from *V. cinerea* were tested for inhibitory activity on coumarin 7-hydroxylation mediated by human recombinant CYP2A6, reconstituted with the rat NADPH-dependent cytochrome P450 reductase (CYPOR) using 2 μM coumarin (close to K_m value) as substrate. Formation of the 7-hydroxycoumarin product was determined at λ_{ex} = 355 nm, λ_{em} = 460 nm [27] using spectrofluorometer (Shimadzu, Kyoto, Japan) The recombinant CYP2A6 and CYPOR enzymes were expressed in *Escherichia coli* and purified as previously described [27,28]. Inhibitory effect was calculated as percent relative inhibition compared with vehicle control reaction and quantified to obtain IC_{50} values (GraphPad Prism 5.0, GraphPad Software Inc, USA).

For determination of the modes of inhibition together with inhibition constant K_i, various final concentrations of coumarin substrate in the range of 0–40 μM and different concentrations of individual test compounds ranging 0–100 μM were used. Modes of inhibition were initially estimated from the Lineweaver–Burk plots and K_i values calculated from the secondary plots using GraphPad Prism 5.0.

Mechanism-based inhibition of CYP2A6 was investigated when the purified compounds caused IC_{50}-shift on CYP2A6 activity [29]. Various concentrations of individual compound (0–40 μM) were pre-incubated at 0, 10, 20, and 30 min in the presence of NADPH, and methoxsalen was used as control mechanism-based inhibitor. The NADPH-dependent inhibition, dialysis, reactions performed with trapping agents (GSH and catalase) and potassium ferricyanide were performed with each of hirsutinolides as previously described [27]. The apparent inactivation constants, K_I and k_{inact}, were calculated from double reciprocal plots of k_{obs} versus inhibitor concentrations by linear regression analysis using GraphPad Prism 5.

2.4. MAO-A and MAO-B assay

The human recombinant microsomal MAO-A and MAO-B enzymes were purchased from Sigma–Aldrich and were employed for inhibition assays using kyuramine as substrate and selegiline as control inhibitor, and assays were conducted as previously described [30]. The formation of 4-hydroxyquinoline product was detected at λ_{ex} = 310 nm and λ_{em} = 400 nm by spectrofluorometer. The inhibition effect was investigated using kynuramine at K_m concentrations for each enzyme (MAO-A = 45 μM and MAO-B = 30 μM). Inhibition effects were calculated as IC_{50} values using GraphPad Prism 5. The inhibition constant (K_i) and modes of inhibition, using various concentrations of kynuramine substrate (0–200 μM for MAO-A and 0–120 μM for MAO-B) was determined with different concentrations of individual test compound (0–100 μM). Those hirsutinolides whose IC_{50} values approaching 100 μM were not further determined modes and kinetics of inhibition. Reactions with 20-min pre-incubation of each purified compounds (2.5–25 μM) performed on MAO-A or MAO-B prior to addition of kynuramine and dialysis experiments were carried out to evaluate whether the inhibition was irreversible [31]. Dialysis was done with pre-incubation reaction mixture at 4 °C for 12 h against 2 L of 100 mM potassium phosphate buffer pH 7.4 containing 22 mM KCl with buffer changed twice during dialysis.

2.5. Statistical analysis

Results were from duplicate or triplicate independent experiments and are shown as means ± standard deviations (SD) in Tables 1–3. Comparison of data in Tables 1–2 and Fig. 3 was statistically analyzed using Student's *t*-test (Statistix 8.0, Analytical Software, Inc., Tallahassee, FL, USA). The results with $p < 0.05$ were considered as significantly difference.

3. Results

Crude EtOH, hexane, EtOAc, and aqueous extracts of *V. cinerea* were investigated inhibition activities against the recombinant human CYP2A6, MAO-A and MAO-B enzymes using fluorescence-based methods, with coumarin as substrate of CYP2A6 and kynuramine as substrate of MAOs. Based on the IC_{50} values, significant inhibition effect (IC_{50} value within 5 μg/ml) was observed against CYP2A6 in EtOH, EtOAc and hexane extracts (Table 1), with more inhibition effect observed in the EtOAc extract than the hexane extract.

In the EtOAc extract, activity-guided purification of inhibitory compounds against CYP2A6 yielded eight compounds. These were three flavones (apigenin, luteolin, and chrysoeriol), one flavonol (quercetin), and four hirsutinolide-type sesquiterpene lactones including 8α-(2-methylacryloyloxy)-hirsutinolide-13-*O*-

Table 1
IC_{50} values, kinetics parameters and mode of inhibition of extracts and purified compounds from *V. cinerea* against CYP2A6.

Samples	IC_{50} value[a,b]		K_i (μM)[a]	K_I (μM)[a,d]	Mode
	Co-incubaition	Pre-incubation			
Ethanol (μg/ml)	4.00 ± 0.14	2.32 ± 0.01[c]	–	–	–
Ethyl acetate fraction(μg/ml)	2.90 ± 0.16	1.57 ± 0.03[c]	–	–	–
Hexane fraction (μg/ml)	3.31 ± 0.24	1.65 ± 0.05[c]	–	–	–
Aqueous fraction (μg/ml)	>100	ND	–	–	–
Flavonoids					
Apigenin (μM)	0.90 ± 0.07	0.77 ± 0.16	0.43 ± 0.17	NA	Mixed-type
Chrysoeriol (μM)	1.14 ± 0.10	0.99 ± 0.12	0.63 ± 0.12	NA	Competitive
Luteolin (μM)	1.38 ± 0.18	1.26 ± 0.07	0.80 ± 0.06	NA	Competitive
Quercetin (μM)	2.66 ± 0.24	2.15 ± 0.38	1.19 ± 0.27	NA	Competitive
Hirsutinolides					
8α-(2-methylacryloyloxy)-hirsutinolide-13-*O*-acetate (μM)	22.3 ± 2.5	8.64 ± 0.37[c]	15.1 ± 2.1	7.45 ± 0.62	Irreversible
8α-(4-hydroxymethacryloyloxy)-hirsutinolide-13-*O*-acetate (μM)	32.7 ± 2.2	6.80 ± 0.77[c]	20.4 ± 5.4	5.32 ± 0.29	Irreversible
8α-tigloloxyhirsutinolide-13-*O*-acetate (μM)	37.8 ± 3.5	20.8 ± 1.1[c]	30.6 ± 1.5	15.4 ± 1.8	Irreversible
8α-(4-hydroxytigloyloxy)-hirsutinolide-13-*O*-acetate (μM)	64.5 ± 5.8	13.1 ± 2.4[c]	42.3 ± 8.4	7.64 ± 1.24	Irreversible

NA = not applicable.
ND = not determined.
[a] Data were obtained from three independent experiments and represent as mean ± SD.
[b] IC_{50} values of methoxsalen (known irreversible inhibitor): 1.53 ± 0.01 μM (co-incubation) and 0.39 ± 0.11 μM (pre-incubation).
[c] Significant difference ($p < 0.05$) between IC_{50} values of co-incubation and pre-incubation.
[d] K_I = inactivation constant as the compound exhibited mechanism-based inhibition pattern.

acetate, 8α-tigloyloxyhirsutinolide-13-*O*-acetate, 8α-(4-hydroxytigloyloxy)-hirsutinolide-13-*O*-acetate, and 8α-(4-hydroxymethacryloyloxy)-hirsutinolide-13-*O*-acetate (Fig. 1). The identities of the isolated compounds were established by comparison of their ^{1}H and ^{13}C NMR spectra and ESI-MS with those previously reported [21–26]. As shown in Table 1, the four flavonoids (IC_{50} values ranging 0.9–2.7 μM) displayed markedly stronger inhibition of CYP2A6 than hirsutinolides, with apigenin exhibited strongest inhibition, followed by chrysoeriol, luteolin, and quercetin. In addition, mechanism-based inhibition (MBI) by these compounds as indication of irreversible inhibition was examined on CYP2A6. The inhibition requires a preceding catalysis process mediated by the enzyme and time to generate a new active inhibitor that reacts with moieties in the active site of enzyme, leading to irreversible loss of enzyme activity [32]. MBI is characterized by NADPH-, concentration- and time-dependent inhibition [32]. Thus pre-incubation of each purified compound with CYP2A6 in the presence or absence of NADPH prior to addition of coumarin substrate at different incubation times was tested. It appeared that there was an increase in inhibition of the four hirsutinolides with increasing pre-incubation time compared with time zero (Fig. 2), while inhibition by all flavonoids was not significantly increased (Table 1). Absence of NADPH in pre-incubation with hirsutinolides abolished time-dependent inhibition pattern (unreported data). The Lineweaver–Burk plots showed that chrysoeriol, luteolin, and quercetin competitively inhibited CYP2A6-mediated coumarin 7-hydroxylation, while apigenin and all hirsutinolides exhibited a mixed-type mode (Table 1, see plots in Supplemental Fig. 1). The K_i values for the four flavonoids (ranging 0.43–1.19 μM) were correlated to their IC_{50} values (Table 1). Hirsutinolides however exerted weaker binding than flavonoids, with K_i values in the

Table 2
Effects of dialysis and potassium ferricyanide on hirsutinolide-mediated inactivation of CYP2A6 activity.

Conditions		Percent remaining activity of CYP2A6[a]
Before dialysis		
(−) Hirsutinolide		100
After dialysis		
(−) Hirsutinolide		92.3 ± 3.6
(+) Hirsutinolides		
25 μM 8α-(2-methylacryloyloxy)-hirsutinolide-13-*O*-acetate,	(−) NADPH	85.6 ± 0.8
25 μM 8α-(2-methylacryloyloxy)-hirsutinolide-13-*O*-acetate,	(+) NADPH	17.9 ± 2.2[b]
25 μM 8α-(4-hydroxymethacryloyloxy)-hirsutinolide-13-*O*-acetate,	(−) NADPH	90.7 ± 1.4
25 μM 8α-(4-hydroxymethacryloyloxy)-hirsutinolide-13-*O*-acetate,	(+) NADPH	31.1 ± 3.3[b]
25 μM 8α-tigloyloxyhirsutinolide-13-*O*-acetate,	(−) NADPH	87.5 ± 0.7
25 μM 8α-tigloyloxyhirsutinolide-13-*O*-acetate,	(+) NADPH	23.0 ± 5.2[b]
25 μM 8α-(4-hydroxytigloyloxy)-hirsutinolide-13-*O*-acetate,	(−) NADPH	88.3 ± 3.0
25 μM 8α-(4-hydroxytigloyloxy)-hirsutinolide-13-*O*-acetate,	(+) NADPH	15.1 ± 2.1[b]
(+) methoxsalen[c]		
2.5 μM methoxsalen,	(−) NADPH	90.2 ± 0.1
2.5 μM methoxsalen,	(+) NADPH	17.9 ± 2.2[b]
70 μM $K_3Fe(CN)_6$		
(+) 25 μM 8α-(2-methylacryloyloxy)-hirsutinolide-13-*O*-acetate,	(+) NADPH	7.9 ± 0.4
(+) 25 μM 8α-(4-hydroxymethacryloyloxy)-hirsutinolide-13-*O*-acetate,	(+) NADPH	6.7 ± 1.5
(+) 25 μM 8α-tigloyloxyhirsutinolide-13-*O*-acetate,	(+) NADPH	22.3 ± 2.8
(+) 25 μM 8α-(4-hydroxytigloyloxy)-hirsutinolide-13-*O*-acetate,	(+) NADPH	12.3 ± 0.8

[a] All values represents mean ± SD and were obtained from duplicate determinations, compared to the reaction without hirsutinolides (before dialysis).
[b] Significant difference between (−) NADPH and (+) NADPH at $p < 0.05$.
[c] Known mechanism-based inhibitor of CYP2A6.

Table 3
IC_{50} values, kinetics parameters and mode of inhibition of extracts and purified compounds from *V. cinerea* toward MAO-A and MAO-B.

Samples	MAO-A[a]			MAO-B[a]		
	IC_{50} value[b]	K_i (μM)[c]	Mode	IC_{50} value[b]	K_i (μM)[c]	Mode
Ethanol (μg/ml)	30.3 ± 1.8	–	–	17.8 ± 1.0	–	–
Ethyl acetate (μg/ml)	15.1 ± 0.8	–	–	14.1 ± 1.3	–	–
Hexane (μg/ml)	43.1 ± 2.8	–	–	23.4 ± 1.7	–	–
Aqueous (μg/ml)	>500	–	–	>500	–	–
Flavonoids						
Apigenin (μM)	0.97 ± 0.08	0.71 ± 0.06	Mixed-type	4.01 ± 0.26	2.24 ± 0.46	Mixed-type
Chrysoeriol (μM)	10.1 ± 0.1	5.64 ± 0.41	Mixed-type	1.25 ± 0.11	0.87 ± 0.04	Mixed-type
Luteolin (μM)	11.5 ± 0.2	6.72 ± 0.70	Mixed-type	25.5 ± 1.9	18.7 ± 1.1	Mixed-type
Quercetin (μM)	3.20 ± 0.08	1.75 ± 0.16	Mixed-type	26.9 ± 0.8	20.8 ± 1.8	Mixed-type
Hirsutinolides						
8α-(2-methylacryloyloxy)-hirsutinolide-13-*O*-acetate (μM)	60.2 ± 1.2	40.4 ± 0.9	Mixed-type	38.6 ± 2.1	27.2 ± 1.3	Mixed-type
8α-tigloyoxyhirsutinolide-13-*O*-acetate (μM)	43.7 ± 0.3	35.6 ± 1.5	Mixed-type	27.3 ± 0.8	23.6 ± 2.5	Mixed-type
8α-(4-hydroxytigloyloxy)-hirsutinolide-13-*O*-acetate (μM)	33.2 ± 1.6	27.7 ± 1.9	Mixed-type	97.3 ± 4.7	ND[d]	ND[d]
8α-(4-hydroxymethacryloyloxy)-hirsutinolide-13-*O*-acetate (μM)	>100	ND[d]	ND[d]	>100	ND[d]	ND[d]

[a] Data were obtained from three independent experiments.
[b] IC_{50} values of selegiline (known selective MAO-B inhibitor) were 31.7 ± 0.3 and 0.052 ± 0.001 μM for MAO-A and MAO-B, respectively.
[c] K_i values of selegiline (known selective MAO-B inhibitor) for MAO-A and MAO-B were 18.9 μM and 0.028 μM, respectively.
[d] ND = not determined due to weak inhibition (IC_{50} value approaching 100 μM).

range of 15.1–42.3 μM (Table 1). To further explore the MBI mode of hirsutinolides and whether any reactive CYP2A6 inactivators formed involved in oxidative radical formation or covalent modification of CYP2A6, experimentations using dialysis, addition of each of trapping agents (GSH and catalase) and potassium ferricyanide in the reaction mixture were performed. Absence of recovery of CYP2A6 activity by dialysis or addition of these chemicals suggested that these hirsutinolides were irreversible inhibitors of CYP2A6 (Table 2 and Fig. 3). Kinetics of inactivation by hirsutinolides (K_I and K_{inact} values) was determined and shown in Fig. 2 and K_I values shown in Table 1.

In the hexane extract, preliminary determination of chemical contents by HPTLC suggested chlorophylls, identified based on their absorbance maxima spectra [33] were major constituent (about 70–80%, data not shown). These chlorophylls, after partially purified from the hexane fraction by TLC and HPLC, showed inhibitory effect on CYP2A6 with the apparent IC_{50} value of 4.46 ± 0.16 μg/ml.

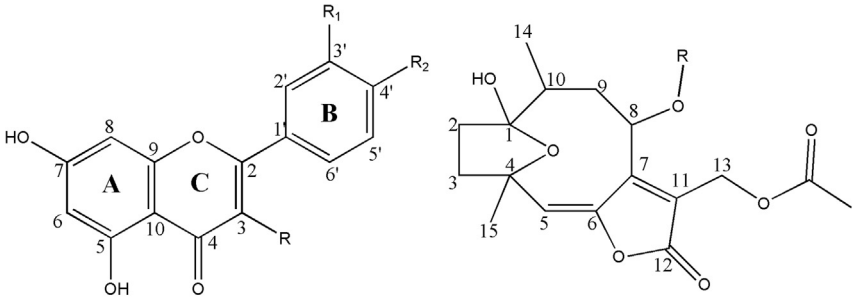

	R_1	R_2	R
1	H	OH	H
2	OCH_3	OH	H
3	OH	OH	H
4	OH	OH	OH

	R
5	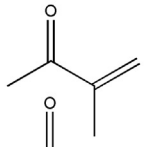
6	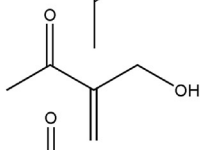
7	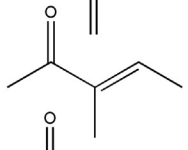
8	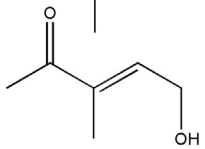

Fig. 1. Chemical structures of flavonoids (1–4) and hirsutinolide-type sesquiterpene lactones (5–8). apigenin (1); chrysoeriol (2); luteolin (3); quercetin (4); 8α-(2-methylacryloyloxy)-hirsutinolide-13-*O*-acetate (5); 8α-(4-hydroxymethacryloyloxy)-hirsutinolide-13-*O*-acetate (6); 8α-tigloyloxyhirsutinolide-13-*O*-acetate (7); 8α-(4-hydroxytigloyloxy)-hirsutinolide-13-*O*-acetate (8).

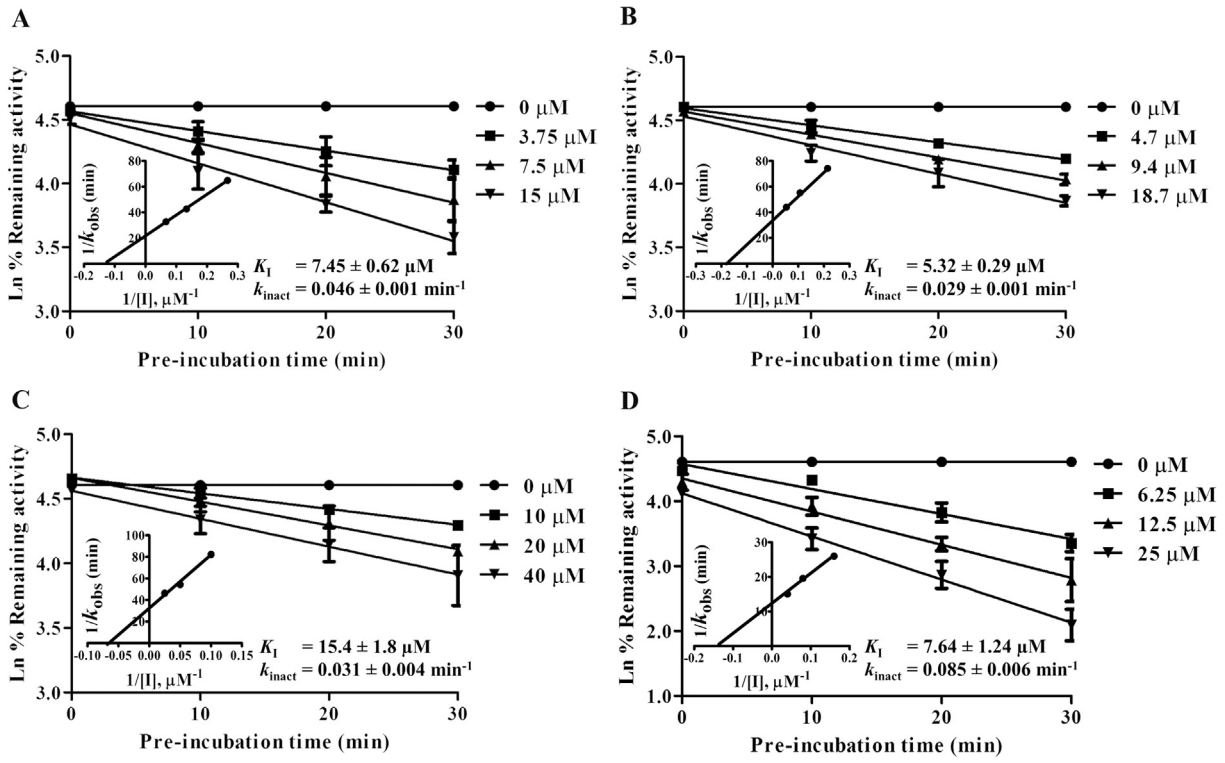

Fig. 2. Time- and concentration-dependent inactivation and kinetics of inhibition of CYP2A6-mediated coumarin 7-hydroxylation by 8α-(2-methylacryloyloxy)-hirsutinolide-13-*O*-acetate (A), 8α-(4-hydroxymethacryloyloxy)-hirsutinolide-13-*O*-acetate (B), 8α-tigloyloxyhirsutinolide-13-*O*-acetate (C), 8α-(4-hydroxytigloyloxy)-hirsutinolide-13-*O*-acetate (D). Various concentrations of each hirsutinolide were used as indicated. Insets represent double-reciprocal plots of k_{obs} values against reciprocal of hirsutinolides. Each data point represents the mean and standard deviation of three independent experiments.

Inhibition effect on human MAOs was observed from EtOH, hexane and EtOAc extracts, but approximately 1.66–2.8 folds less inhibition was observed with hexane extract than EtOAc extract (Table 3). Activity-guided purification of compounds in EtOAc extract against MAO-A and MAO-B essentially yielded the same flavonoids as for CYP2A6. Regarding IC_{50} values, chrysoeriol was the strongest inhibitor against MAO-B, while apigenin was the most potent inhibitor against MAO-A (Table 3). The hirsutinolides inhibited and bound to MAOs with varying degrees, with less inhibition potential on MAO-A than flavonoids. However MAO-B was preferably bound by 8α-(2-methylacryloyloxy)-hirsutinolide-13-*O*-acetate and 8α-tigloyoxyhirsutinolide-13-*O*-acetate, with binding (K_i) values relatively comparable to luteolin and quercetin (Table 3). A 20 min pre-incubation with these flavonoids and hirsutinolides did not increase inhibition against both human MAOs and activities of both MAOs could be recovered after dialysis (unreported data), indicating absence of MBI inhibition [31] and their inhibitions were reversible. Lineweaver–Burk plots showed that flavonoids and hirsutinolides inhibited both MAOs in mixed-type mode (Table 3, Supplemental Figs. 2 and 3). In the hexane fraction, we observed that chlorophylls might be a major contributor to inhibition of MAOs, since partially purified chlorophylls showed inhibitory effect on MAO-A and MAO-B with apparent IC_{50} values of 19.8 ± 1.1 and 10.9 ± 1.0 μg/ml, respectively.

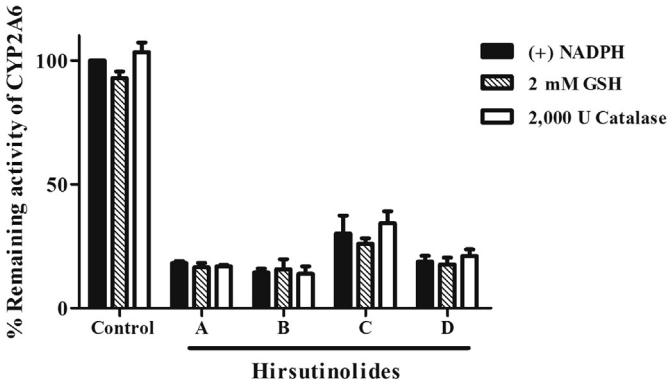

Fig. 3. Effects of trapping agents on inactivation of recombinant CYP2A6 by 8α-(2-methylacryloyloxy)-hirsutinolide-13-*O*-acetate (A), 8α-(4-hydroxymethacryloyloxy)-hirsutinolide-13-*O*-acetate (B), 8α-tigloyloxyhirsutinolide-13-*O*-acetate (C), 8α-(4-hydroxytigloyloxy)-hirsutinolide-13-*O*-acetate (D). CYP2A6 was pre-incubated with hirsutinolides (25 μM) for 10 min in the presence and absence of trapping agents. The percent remaining activity of CYP2A6 was measured. Each column represents the mean ± SD of duplicate determinations. Reaction in the absence of hirsutinolides and trapping agents was set to 100 percent remaining activity.

4. Discussion

V. cinerea has a wide range of pharmacological activities and has been commonly used in traditional medicine for various treatments such as cough, asthma, bronchitis [17]. Tea preparations of *V. cinerea* administered prior to smoking was reported ability to reduce smoking rate in smokers [19,20]. It was suggested that *V. cinerea* generated unpleasant taste and smell of cigarette smoke, leading to reduced cigarette craving in smokers [19]. However the mechanisms underlying nicotine abstinence of *V. cinerea* and its active constituents on two pharmacotherapeutic targets of tobacco dependence, nicotine and dopamine metabolisms, have not been reported. The present study revealed potential inhibitory effect of *V. cinerea* extract and its active constituents on the human CYP2A6, MAO-A and MAO-B enzymes *in vitro*, suggesting that modulation of

nicotine and dopamine metabolisms by *V. cinerea* could be liable for smoking abstinence effects of *V. cinerea*.

Preliminary determination by HPLC and TLC of compounds in *V. cinerea* EtOH extract compared with compounds in tea prepared according to the previously described protocol [20] gave approximately similar patterns of HPLC and TLC chromatograms, suggesting similar active compounds were existed in both preparations (data not shown). Activity-guided isolation of active compounds from the EtOAc extract of *V. cinerea* indicated that flavonoids and hirsutinolides were contributors to CYP2A6 inhibition, while inhibition by the hexane extract could be explained by the presence of most chlorophylls in the extract. Non-specific inhibition of chlorophyllin, a copper/sodium salt of chlorophyll, toward CYPs including CYP2A6 has also been shown [34], but inhibition toward MAOs has not been reported. Other unidentified compounds could also be responsible for inhibition effect in the hexane fraction. However our results could infer that chlorophylls exerted notable inhibition effects on both nicotine and dopamine metabolisms.

In the EtOAc fraction, eight purified compounds including four flavonoids and four hirsutinolide-type sesquiterpene lactones were isolated. The four flavonoids of *V. cinerea* comprised high degree of reversible inhibition on CYP2A6 with K_i values within 1.5 μM range (K_i values of apigenin, chrysoeriol, luteolin, and quercetin were 0.43, 0.63, 0.8, 1.19 μM, respectively, Table 1). Judging from K_i values, they were more or less comparable to known CYP2A6 inhibitors, including tryptamine, phenethyl isothiocyanate, menthofuran, and pilocarpine (K_i values of 1.7, 1.7, 2.0, and 3 μM, respectively), but were less effective than methoxalen whose K_i value was 0.25 μM [35]. The flavonoids obtained in this study comprised multiple hydroxyl groups at specific positions in the A and B rings (Fig. 1) and might be influential to CYP2A6 inhibition. These included hydroxyl groups at 4′,5,7 and 3′4′,5,7 positions in apigenin and luteolin, respectively, or 3′-methoxy group in addition to 4′,5,7-hydroxyl groups (in case of chrysoeriol). When two flavones without hydroxyl group in the B ring, chrysin (5,7-dihydroxyflavone) and wogonin (5,7-dihydroxy-8-methoxyflavone) which are commonly found in various plants were tested, their inhibition in the mixed-type mode (K_i values of 2.91 ± 0.54 and 5.03 ± 0.92 μM, respectively) were markedly less potent than apigenin by 6.8 and 11.7 folds (data not shown). These results suggested the importance of hydroxyl and/or methoxy groups in the B ring of flavones on potency of CYP2A6 inhibition. Therefore flavonoids found in *V. cinerea* were those effectively inhibited CYP2A6 enzyme. Numbers and positions of hydroxyl and/or methoxy groups of various flavonoids have also been found highly impact on inhibition potential of flavonoids toward various human CYPs [36].

Four hirsutinolides showed MBI and were irreversible inhibitors of CYP2A6, as revealed by their time-, concentration-, and NADPH-dependent inhibition pattern (Fig. 2), and the inhibition could not be reversed by dialysis, presence of trapping agents or potassium ferricyanide (Table 2). Judging from K_I values of previously reported MBI inhibitors of CYP2A6, including methoxsalen, menthofuran, decursinol angelate, rhinacanthin-A, -B, and -C that had K_I values of 0.8, 2.2, 2.42, 0.69, 0.44, and 0.97 μM, respectively [27,37–39], these hirsutinolides with K_I values ranging 5.32–15.4 μM were weaker inactivators but were more or less stronger than selegiline whose K_I value was 15.6 μM [40]. Irreversible inhibition of human CYPs by hirsutinolides has not been reported, whether they are selective inhibitors of CY2A6 remains to be investigated by inhibition studies with other human P450 isoforms. Luteolin and 8α-tigloyloxyhirsutinolide-13-*O*-acetate, found in highest amount among the active flavonoids and hirsutinolides, respectively, were also found inhibited CYP2A6-mediated nicotine metabolism (Supplemental Fig. 4). Moreover 8α-tigloyloxyhirsutinolide-13-*O*-acetate had higher inhibitory activity upon pre-incubation than co-incubation condition against nicotine metabolism (Supplemental Fig. 4) in consistent with the results of coumarin 7-hydroxylation inhibition assays, implicating that these *V. cinerea* flavonoids and hirsutinolides could inhibit nicotine metabolism catalyzed by CYP2A6. The potential inhibitory effects of flavonoids as reversible inhibitors combined with irreversible inactivation of CYP2A6 by hirsutinolides might contribute to smoking abstinence in smokers drinking *V. cinerea* tea prior to smoking.

Inhibition of MAOs by synthetic compounds and various flavonoids as natural plant products were reported [41]. In *V. cinerea*, inhibition of the four hirsutinolides against human MAO-A were inferior to flavonoids (Table 3). In contrast based on K_i values, 8α-(2-methylacryloyloxy)-hirsutinolide-13-*O*-acetate and 8α-tigloyoxyhirsutinolide-13-*O*-acetate were relatively comparable to luteolin and quercetin flavonoids in inhibition against human MAO-B, implicating that the two hirsutinolides were contributors of human MAO-B inhibition (Table 3).

Compared among IC_{50} values of flavonoids obtained from *V. cinerea* against human MAOs, apigenin, quercetin and luteolin were more active toward MAO-A (IC_{50} values of 0.97, 3.20, 11.5 μM, respectively against MAO-A and 4.01, 26.92, and 25.5 μM, respectively against MAO-B, Table 3), while chrysioeriol more potently inhibited MAO-B, with approximately 8-fold selectivity toward MAO-B (IC_{50} values of 10.1 and 1.25 μM against MAO-A and MAO-B, respectively, Table 3). Prior studies of MAOs in mouse indicate that increase of hydroxyl groups in the B ring of flavonoids, absence of C2–C3 double bond (seen for flavanones and flavanols), or introduction of glucose at C7 in flavonoids could decrease MAO inhibition [42]. This thus explained that apigenin with one hydroxyl group in the B ring displayed about 3.2–11.8 folds more inhibition against human MAOs in this study than luteolin and quercetin whose B ring contained 3′,4′-hydroxyl groups. Flavanols with the absence of C2–C3 double bond such as catechin and epicatechin also possess less inhibition potential, judging from IC_{50} values of 88.6 and 58.9 μM, respectively against rat MAO-B [43] than flavones and 8α-(2-methylacryloyloxy)-hirsutinolide-13-*O*-acetate and 8α-tigloyoxyhirsutinolide-13-*O*-acetate against human MAOs reported herein. Notably, insertion of 3′-methoxy group in the B ring of chrysoeriol could be important, rendering about 3.2 folds stronger binding to MAO-B than apigenin as referring to K_i values. Comparing to inhibition of human MAOs by harman (IC_{50} values of 0.34 μM against MAO-A and >100 μM toward MAO-B) and norharman (values of 6.47 μM on MAO-A and 4.68 μM on MAO-B) β-carboline alkaloids that were found in cigarette smoke, these flavonoids inhibited both MAOs with comparable potential [5]. To our knowledge, the present study reports for the first time that chrysoeriol effectively inhibited human MAO-B and CYP2A6. The results could have an implication for its development of a therapeutic lead from natural source to facilitate smoking cessation through its combined effects on nicotine and dopamine metabolisms.

In summary, this is the first report of identification of flavonoids and hirsutinolides active compounds from *V. cinerea* that displayed inhibition potentials toward therapeutic targets of tobacco dependence, CYP2A6, MAO-A and MAO-B, and their inhibition kinetics were characterized. Other mechanisms that interrupt nicotine action manifested by these flavonoids and hirsutinolides or other *V. cinerea* active compounds remain to be elucidated. Moreover *V. cinerea* herbal ingredients with the absence of toxic effects in mice [44] might be of interest as other molecular targets for relieving tobacco dependence have yet to be investigated. The results of the present study could also have implications in combination of drug therapy for smoking cessation, in particular chrysoeriol was shown a potent dual human MAO-B/CYP2A6 inhibitor.

Acknowledgements

This work was supported by the Development and Promotion of Science and Technology Talents Project (DPST), Thailand, Thailand Research Fund (TRF) grant number TRG 5780056 and Burapha University 34/2558, the Central Instrument Facility (CIF) (CIF 57/028), Research Division, Faculty of Science, Mahidol University.

Appendix A. Supplementary data

Supplementary data related to this article can be found at http://dx.doi.org/10.1016/j.dmpk.2014.12.005.

References

[1] Benowitz NL. Pharmacology of nicotine: addiction, smoking-induced disease, and therapeutics. Annu Rev Pharmacol Toxicol 2009;49:57–71.
[2] Messina DS, Tyndale RF, Sellers EM. A major role for CYP2A6 in nicotine C-oxidation by human liver microsomes. J Pharmacol Exp Ther 1997;282:1608–14.
[3] Yamazaki H, Inui Y, Yun CH, Guengerich FP, Shimada T. Cytochrome P4502E1 and 2A6 enzyme as major catalysts for metabolic activation of *N*-nitrosodialkyl-amines and tobacco-related nitrosamine in human liver microsomes. Carcinogenesis 1992;13:1789–94.
[4] Fowler JS, Logan J, Wang GJ, Volkow ND. Monoamine oxidase and cigarette smoking. Neurotoxicology 2003;24:75–82.
[5] Herraiz T, Chaparro C. Human monoamine oxidase is inhibited by tobacco smoke: beta-carboline alkaloids act as potent and reversible inhibitors. Biochem Biophys Res Commun 2005;326:378–86.
[6] Rose JE, Behm FM, Ramsey C, Ritchie Jr JC. Platelet monoamine oxidase, smoking cessation, and tobacco withdrawal symptoms. Nicotine Tob Res 2001;3:383–90.
[7] Gilbert DG, Zuo Y, Browning RA, Shaw TM, Rabinovich NE, Gilbert-Johnson AM, et al. Platelet monoamine oxidase B activity changes across 31 days of smoking abstinence. Nicotine Tob Res 2003;5:813–9.
[8] Zhang L, Dong Y, Doyon WM, Dani JA. Withdrawal from chronic nicotine exposure alters dopamine signaling dynamics in the nucleus accumbens. Biol Psychiatry 2012;71:184–9.
[9] Siu EC, Tyndale RF. Non-nicotinic therapies for smoking cessation. Annu Rev Pharmacol Toxicol 2007;47:541–64.
[10] Lerman C, Tyndale R, Patterson F, Wileyto EP, Shields PG, Pinto A, et al. Nicotine metabolite ratio predicts efficacy of transdermal nicotine for smoking cessation. Clin Pharmacol Ther 2006;79:600–8.
[11] Sellers EM, Kaplan HL, Tyndale RF. Inhibition of cytochrome P450 2A6 increases nicotine's oral bioavailability and decreases smoking. Clin Pharmacol Ther 2000;68:35–43.
[12] Sellers EM, Ramamoorthy Y, Zeman MV, Djordjevic MV, Tyndale RF. The effect of methoxsalen on nicotine and 4-(methylnitrosamino)-1-(3-pyridyl)-1-butanone (NNK) metabolism. In Vivo Nicotine Tob Res 2003;5:891–9.
[13] Houtsmuller EJ, Thornton JA, Stitzer ML. Effects of selegiline (L-deprenyl) during smoking and short-term abstinence. Psychopharmacology 2002;163:213–20.
[14] Biberman R, Neumann R, Katzir I, Gerber Y. A randomized controlled trial of oral selegiline plus nicotine skin patch compared with placebo plus nicotine skin patch for smoking cessation. Addiction 2003;98:1403–7.
[15] George TP, Vessicchio JC, Termine A, Jatlow PI, Kosten TR, O'Malley SS. A preliminary placebo-controlled trial of selegiline hydrochloride for smoking cessation. Biol Psychiatry 2003;53:136–43.
[16] Berlin I, Saïd S, Spreux-Varoquaux O, Launay JM, Olivares R, Millet V, et al. A reversible monoamine oxidase a inhibitor (moclobemide) facilitates smoking cessation and abstinence in heavy, dependent smokers. Clin Pharmacol Ther 1995;58:444–52.
[17] Toyang NJ, Verpoorte R. A review of the medicinal potentials of plants of the genus *Vernonia* (Asteraceae). J Ethnopharmacol 2013;146:681–723.
[18] Iwalewa EO, Iwalewa OJ, Adeboye JO. Analgesic, antipyretic, anti-inflammatory effects of methanol, chloroform and ether extracts of *Vernonia cinerea* less leaf. J Ethnopharmacol 2003;86:229–34.
[19] Wongwiwatthananukit S, Benjanakaskul P, Songsak T, Suwanamajo S, Verachai V. Efficacy of *Vernonia cinerea* for smoking cessation. J Health Res 2009;23:31–6.
[20] Leelarungrayub D, Pratanaphon S, Pothongsunun P, Sriboonreung T, Yankai A, Bloomer RJ. *Vernonia cinerea* Less. supplementation and strenuous exercise reduce smoking rate: relation to oxidative stress status and beta-endorphin release in active smokers. J Int Soc Sports Nutr 2010;26:7–21.
[21] Cowall PL, Cassady JM, Chang C, Kozlowski JF. Isolation and structure determination of piptocarphins A-F, cytotoxic germacranolide lactones from *Piptocarpha chontalensis*. J Org Chem 1981;46:1108–14.
[22] Kuo YH, Kuo YJ, Yu AS, Wu MD, Ong CW, Yang- Kuo LM, et al. Two novel sesquiterpene lactones, cytotoxic vernolide-A and -B, from *Vernonia cinerea*. Chem Pharm Bull 2003;51:425–6.
[23] Chen X, Zhan ZJ, Zhang XW, Ding J, Yue JM. Sesquiterpene lactones with potent cytotoxic activities from *Vernonia chinensis*. Planta Med 2005;71:949–54.
[24] Plazonić A, Bucar F, Males Z, Mornar A, Nigović B, Kujundzić N. Identification and quantification of flavonoids and phenolic acids in burr parsley (*Caucalis platycarpos* L.), using high-performance liquid chromatography with diode array detection and electrospray ionization mass spectrometry. Molecules 2009;14:2466–90.
[25] Kang J, Li Z, Wu T, Jensen GS, Schauss AG, Wu X. Anti-oxidant capacities of flavonoid compounds isolated from acai pulp (*Euterpe oleracea* Mart.). Food Chem 2010;122:610–7.
[26] Youn UJ, Park EJ, Kondratyuk TP, Simmons CJ, Borris RP, Tanamatayarat P, et al. Anti-inflammatory sesquiterpene lactones from the flower of *Vernonia cinerea*. Bioorg Med Chem Lett 2012;22:5559–62.
[27] Pouyfung P, Prasopthum A, Sarapusit S, Srisook E, Rongnoparut P. Mechanism-based inactivation of cytochrome P450 2A6 and 2A13 by *Rhinacanthus nasutus* constituents. Drug Metab Pharmacokinet 2014;29:75–82.
[28] Soucek P. Expression of cytochrome P450 2A6 in *Escherichia coli*: purification, spectral and catalytic characterization, and preparation of polyclonal antibodies. Arch Biochem Biophys 1999;370:190–200.
[29] Hollenberg PF, Kent UM, Bumpus NN. Mechanism-based inactivation of human cytochromes p450s: experimental characterization, reactive intermediates, and clinical implications. Chem Res Toxicol 2008;21:189–205.
[30] Mostert S, Ment ZW, Petzer A, Bergh JJ, Petzer JP. Inhibition of monoamine oxidase by 8-[(phenylehtyl)sulfanyl]caffeine analogues. Bioorg Med Chem 2012;20:7040–50.
[31] Fowler CJ, Mantle TJ, Tipton KF. The nature of the inhibition of rat liver monoamine oxidase types A and B by the acetylenic inhibitors clorgyline, l-deprenyl and pargyline. Biochem Pharmacol 1982;31:3555–61.
[32] Correia MA, Ortiz de Montello PR. Inhibition of cytochrome P450 enzymes. In: Montello PR, editor. Cytochrome P450: structure, mechanism, and biochemistry. New York: Kluwer Academic/Plenym Publishers; 2005. p. 247–332.
[33] Almela L, Fernández-López JA, Roca MJ. High-performance liquid chromatographic screening of chlorophyll derivatives produced during fruit storage. J Chromatogr A 2000;870:483–9.
[34] Yun CH, Jeong HG, Jhoun JW, Guengerich FP. Non-specific inhibition of cytochrome P450 activities by chlorophyllin in human and rat liver microsomes. Carcinogenesis 1995;16:1437–40.
[35] Stephens ES, Walsh AA, Scott EE. Evaluation of inhibition for human cytochrome P450 2A enzymes. Drug Metab Dispos 2012;40:1797–802.
[36] Shimada T, Tanaka K, Takenaka S, Murayama N, Martin MV, Foroozesh MK, et al. Structure-function relationships of inhibition of human cytochromes P450 1A1, 1A2, 1B1, 2C9, and 3A4 by 33 flavonoid derivatives. Chem Res Toxicol 2010;23:1921–35.
[37] Koenigs LL, Peter RM, Thompson SJ, Rettie AE, Trager WF. Mechanism-based inactivation of human liver cytochrome P450 2A6 by 8-methoxypsoralen. Drug Metab Dispos 1997;25:1407–15.
[38] Khojasteh-Bakht SC, Koenigs LL, Peter RM, Trager WF, Nelson SD. (R)-(+)-Menthofuran is a potent, mechanism-based inactivator of human liver cytochrome P450 2A6. Drug Metab Dispos 1998;26:701–4.
[39] Yoo HH, Lee MW, Kim YC, Yun C, Kim DH. Mechanism-based inactivation of cytochrome P450 2A6 by decursinol angelate isolated from *Angelica gigas*. Drug Metab Dispos 2007;35:1759–65.
[40] Siu EC, Tyndale RF. Selegiline is a mechanism-based inactivator of CYP2A6 inhibition nicotine metabolism in humans and mice. J Pharmacol Exp Ther 2008;324:992–9.
[41] Carradori S, D'Ascenzio M, Chimenti P, Secci D, Bolasco A. Selective MAO-B inhibitors: a lesson from natural products. Mol Divers 2014;18:219–43.
[42] Han XH, Hong SS, Hwang JS, Lee MK, Hwang BY, Ro JS. Monoamine oxidase inhibitory components from *Cayratia japonica*. Arch Pharm Res 2007;30:13–7.
[43] Hou WC, Lin RD, Chen CT, Lee MH. Monoamine oxidase B (MAO-B) inhibition by active principles from *Uncaria rhynchophyla*. J Ethnopharmacol 2005;100:216–20.
[44] Latha LY, Darah I, Jain K, Sasidharan S. Toxicity study of *Vernonia cinerea*. Pharm Biol 2010;48:101–4.